5A.5 AN OBSERVATIONAL ANALYSIS OF Z_{DR} COLUMN TRENDS IN TORNADIC SUPERCELLS

Joseph C. Picca[1]*, Jeffrey C. Snyder[2], and Alexander V. Ryzhkov[2]

[1]*NOAA/NWS/NCEP/Storm Prediction Center, Norman, OK*

[2]*Cooperative Institute for Mesoscale Meteorological Studies, University of Oklahoma, Norman, OK*

1. Introduction

Within the updraft of a thunderstorm cell, liquid drops can be lofted several kilometers above the height of the environmental freezing level (EFL). If the upward vertical motion is sufficient, lofted drops may rapidly accumulate mass via coalescence. The oblate shape of such drops contributes positively to differential reflectivity $Z_{DR.}$ In turn, the positive thermal perturbation from latent heating within the updraft favors a region of enhanced Z_{DR} above the EFL. Moreover, non-instantaneous freezing of drops (e.g., Pruppacher and Klett 1997; Kumjian et al. 2012) can yield an upward extension of this enhancement, such that a vertically continuous column forms. Thus, this signature is known as the "Z_{DR} column" and has been frequently reported within the literature (e.g., Hall et al.1984; Illingworth et al. 1987; Caylor and Illingworth 1987). Typically at S band, Z_{DR} values within this signature range from around 1 to 3 dB, with occasional values as high as 5 dB. An example of a Z_{DR} column is provided in Fig. 1.

The recent deployment of polarimetric capability to the WSR-88D fleet offers a valuable opportunity to observe, track, and predict convective updrafts on a broad scale. Indeed, Kumjian et al. (2014) and Snyder et al. (2015) show via a 2-D cloud model with bin (spectral) microphysics that a positive correlation exists between the column depth and updraft strength.

Thus, as these columns are inextricably linked with storm cell updrafts, a natural extension of their observation is the relation between their evolution and storm-scale dynamic and kinematic processes.

2. Z_{DR} Column Trends and Tornadogenesis

One topic of exploration is the potential link between Z_{DR} column trends prior to, during, and after tornadogenesis. Previous work has suggested that mid-level updraft intensity may weaken prior to tornadogenesis, owing to an increased downward-directed pressure perturbation gradient force as the low-level mesocyclone strengthens (e.g., Brandes

* *Corresponding author address:* Joseph C. Picca, Storm Prediction Center, National Weather Center, 120 David L. Boren Blvd., Ste. 2300, Norman, OK 73072; joey.picca@noaa.gov

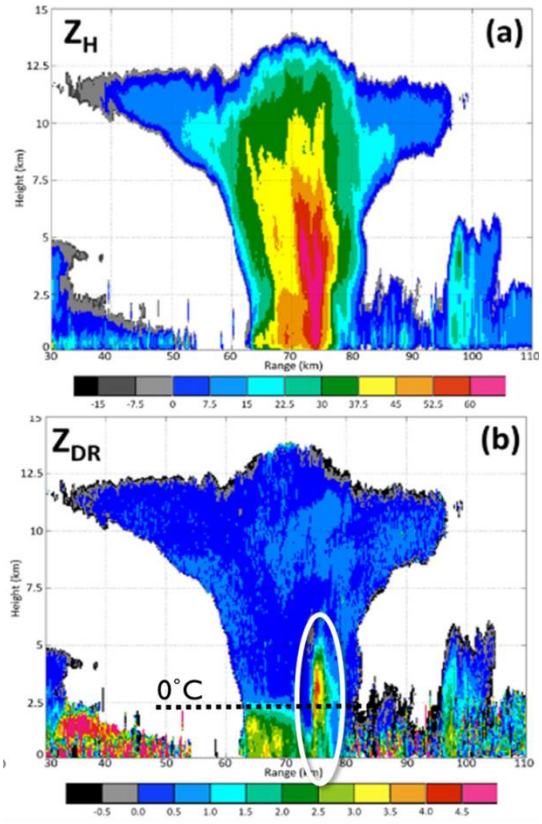

Fig. 1: RHI of (a) Z_H and (b) Z_{DR} from a convective cell (Kumjian et al. 2014). Note the Z_{DR} column around 75 km in range.

1978; Lemon and Doswell 1979; Houze 1993; Adlerman et al. 1999; Trapp 1999). Considering the positive correlation between Z_{DR} column height and updraft strength, one may reasonably expect that the column height may decrease prior to supercellular tornadogenesis (Fig. 2). In turn, the potential would exist for gleaning prognostic capabilities from the trends of Z_{DR} column depths with regard to tornadic development.

2.1 Z_{DR} Column Algorithm

While Picca et al. (2010) performed a preliminary analysis of such trends in a small sample of three tornadic supercells, the advent of the Z_{DR} Column Algorithm (Snyder et al. 2015) provides an opportunity to examine more cases efficiently. After pre-processing polarimetric single-radar data (see Snyder et al. 2015 for details), the algorithm outputs the depth of a detected Z_{DR} column by identifying vertically continuous grids with $Z_{DR} \geq 1$ dB above the environmental 0˚C level (from the Rapid Refresh model). Certainly, several caveats exist with such an approach to Z_{DR} column detection and quantification, but the reader is directed to Snyder et al. (2015) for more information on the topic. Furthermore, this algorithm stands as the first automated method for monitoring Z_{DR} column depth in an operational setting, and thus offers significant promise for improving forecasters' situational awareness of storm-cell evolution.

2.2 Methodology

Potential cases across the WSR-88D network over the period of March – June 2014 were considered. Additionally, supercell tornadoes that occurred more than 100 km away from the closest radar were not included, as degraded vertical radar resolution would negatively impact this study. Forty-five supercell tornado cases were identified and suitable for quantitative analysis (i.e., the algorithm output was not detrimentally impacted by signal depolarization, poor vertical sampling, etc.). For each of these cases, the Z_{DR} column associated with the parent updraft of the tornado was identified near the time of

tornadogenesis. The column was then subjectively tracked backwards for up to 30 min prior to tornadogenesis or until the column could no longer be identified, whichever occurred first. The maximum column height for each volume scan was then recorded through the time of tornado dissipation.

An example of the cases is provided in Fig. 3. At 0239 UTC on 29 April 2014, a tornado developed from a discrete supercell in Cullman Co., Alabama. The tornado persisted for approximately 20 minutes and produced up to EF-3 damage during its lifespan. In the minutes leading up to tornado development, Z_{DR} column heights of 2.93 – 3.60 km above the EFL are exhibited by the algorithm. Following tornado development, the algorithm depicts Z_{DR} column heights of 2.03 – 2.30 km above the EFL. This information was recorded for all 45 cases, and the results are supplied in the following section. Moreover, the tornadoes were categorized by damage intensity: weak (EF-0 – EF-1; 27 cases) and significant (EF-2+; 18 cases).

3. Results and Analysis

Evident in Fig. 4, there was little to no signal regarding the evolution of the maximum height of the column prior to or after tornadogenesis for weak tornadoes. While there may be a minor tendency for a decrease of a few hundred meters per five minutes around 0-10 min prior to tornadogenesis, numerous cases exhibit increasing column heights leading up to the tornado start time. Furthermore, at even earlier times, as well as times after tornadogenesis, the distribution is generally centered on a value of 0 (i.e., no change). Table 1 provides more details of the trends for weak and significant tornadoes prior to their development. Indeed, 9 (10) weak-tornado cases exhibit increasing heights between 10 and 5 minutes (5 and 0 minutes) prior to tornadogenesis. Additionally, while a greater percentage of cases exhibits decreasing column heights in the 10-to-0-min range, the mean decrease is only around 500 m. Thus, these cases appear to provide little support for our hypothesis that Z_{DR} columns weaken prior to tornadic development.

While lacking a strong signal as well, the second set of data (significant tornadoes) exhibits at least a greater tendency for decreasing column heights (generally on the order of 200 – 500 m [5 min]$^{-1}$) prior to and after tornadogenesis. As stronger tornadoes are likely associated with stronger low-level mesocyclones, one may reasonably surmise that the downward-directed pressure perturbation gradient force is also greater in these cases than it is with weak tornadoes. In turn, column heights may be more likely to decrease prior to tornadogenesis for these cases. While Table 1 indicates that several cases still exhibit increasing Z_{DR} columns prior to tornadogenesis, the mean increase for each time period is generally lower than those for weak-tornado cases. These trends are at least slightly more supportive of the hypothesis than

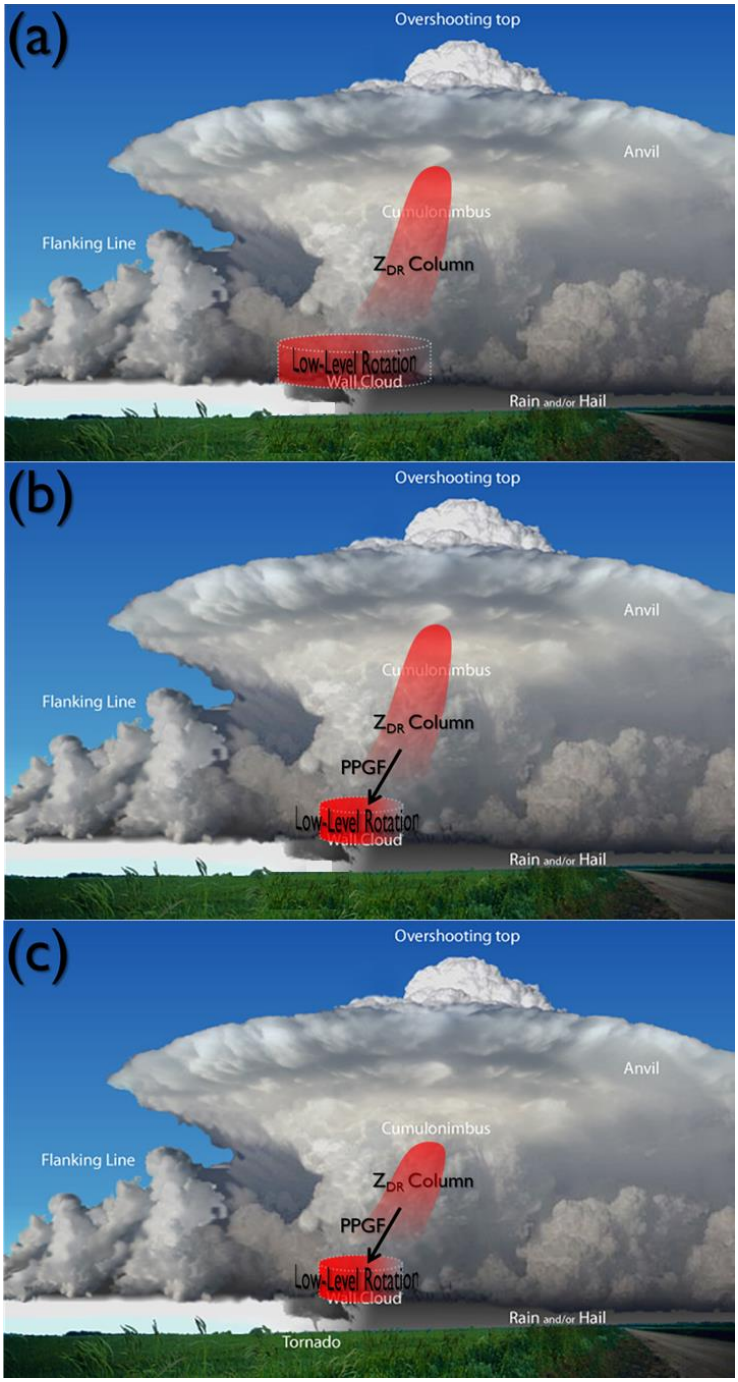

Fig. 2: A conceptual model of the hypothesis of weakening Z_{DR} columns prior to supercellular tornadogenesis. As low-level rotation strengthens from (a) to (b), a downward-directed perturbation pressure gradient force develops. In response, (c) the depth of the Z_{DR} column decreases near/prior to tornadogenesis.

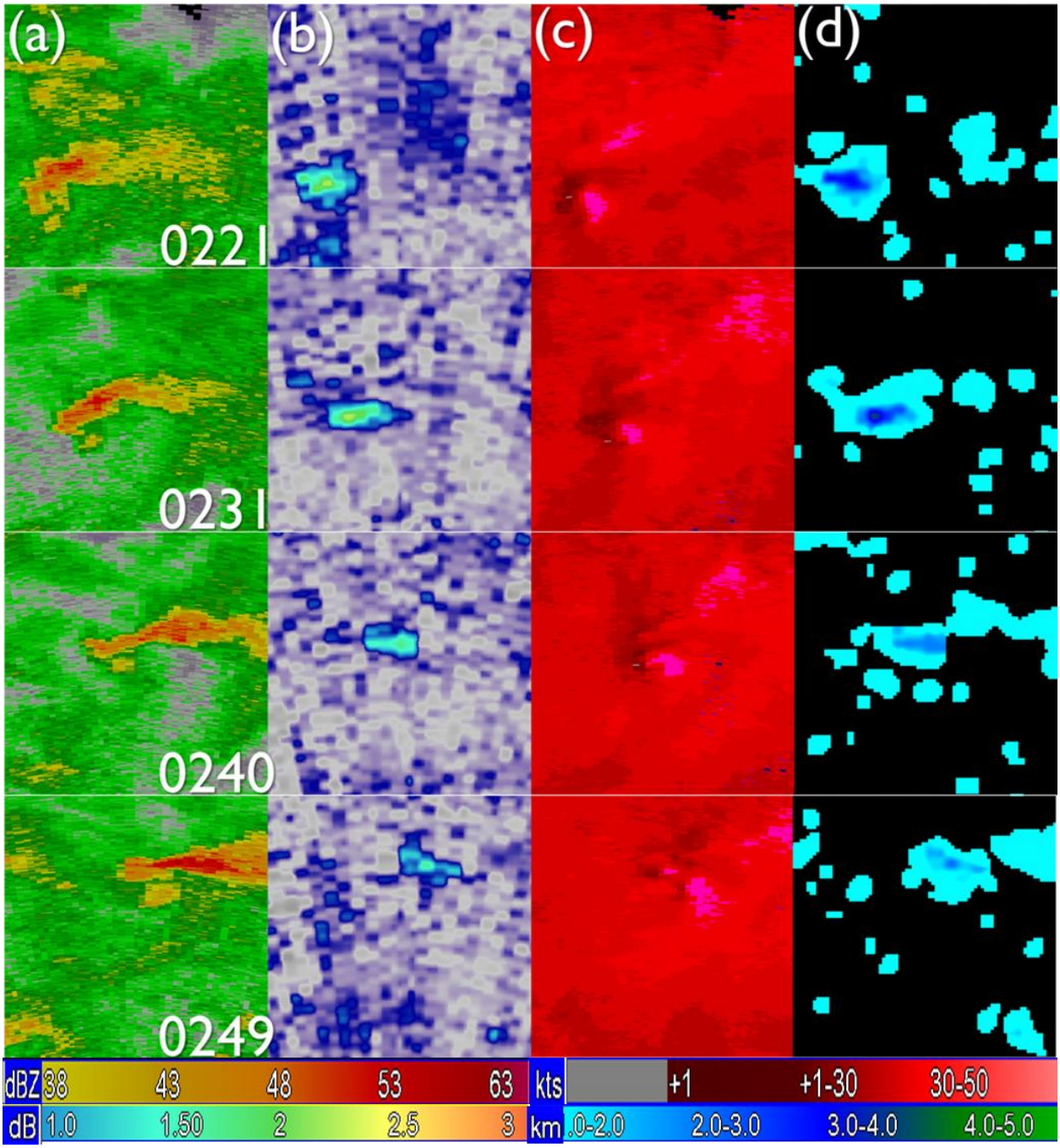

Fig. 3: a) 0.5˚ reflectivity Z_H PPI (scale upper-left), b) 5-km AGL differential reflectivity Z_{DR} CAPPI (scale lower-left), c) 0.5˚ base velocity (scale upper-right), and d) Z_{DR} column algorithm output (scale lower-right) from KBMX on 29 April 2014. A tornado developed from this supercell at 0239 UTC. Note the decrease in Z_{DR} column height after 0231 UTC.

those for the weak tornadoes. Additionally, the higher intensity and greater longevity of the tornadoes in these cases suggest persistence and/or strengthening of the low-level mesocyclone intensity after tornadogenesis. Thus, the continuation of the slightly negative height trends after

tornado development (Fig. 4) is consistent with the hypothesis as well.

4. Conclusion and Future Work

Z_{DR} columns offer a valuable opportunity to identify and track convective updrafts, enhancing forecasters' ability to predict near-term trends in storm intensity. Moreover, this signature facilitates comparison of storm-scale processes (e.g., tornadogenesis) with changes in updraft characteristics.

While this dataset, at best, only weakly supports the hypothesis of decreasing Z_{DR} column depth prior to tornadogenesis, we theorize that several factors may have precluded a stronger signal. Chiefly, the relatively poor vertical resolution of the WSR-88D scan strategies can be rather detrimental to Z_{DR} column detection, especially at distant ranges from the radar. Thus, sampling of these columns may often be inadequate for the quantitative purposes of this study. Moreover, artifacts such as depolarization can artificially increase or decrease the column height, and radar miscalibration can also prove harmful to algorithm performance.

Despite these challenges, several avenues for further work remain and could bolster the current argument.

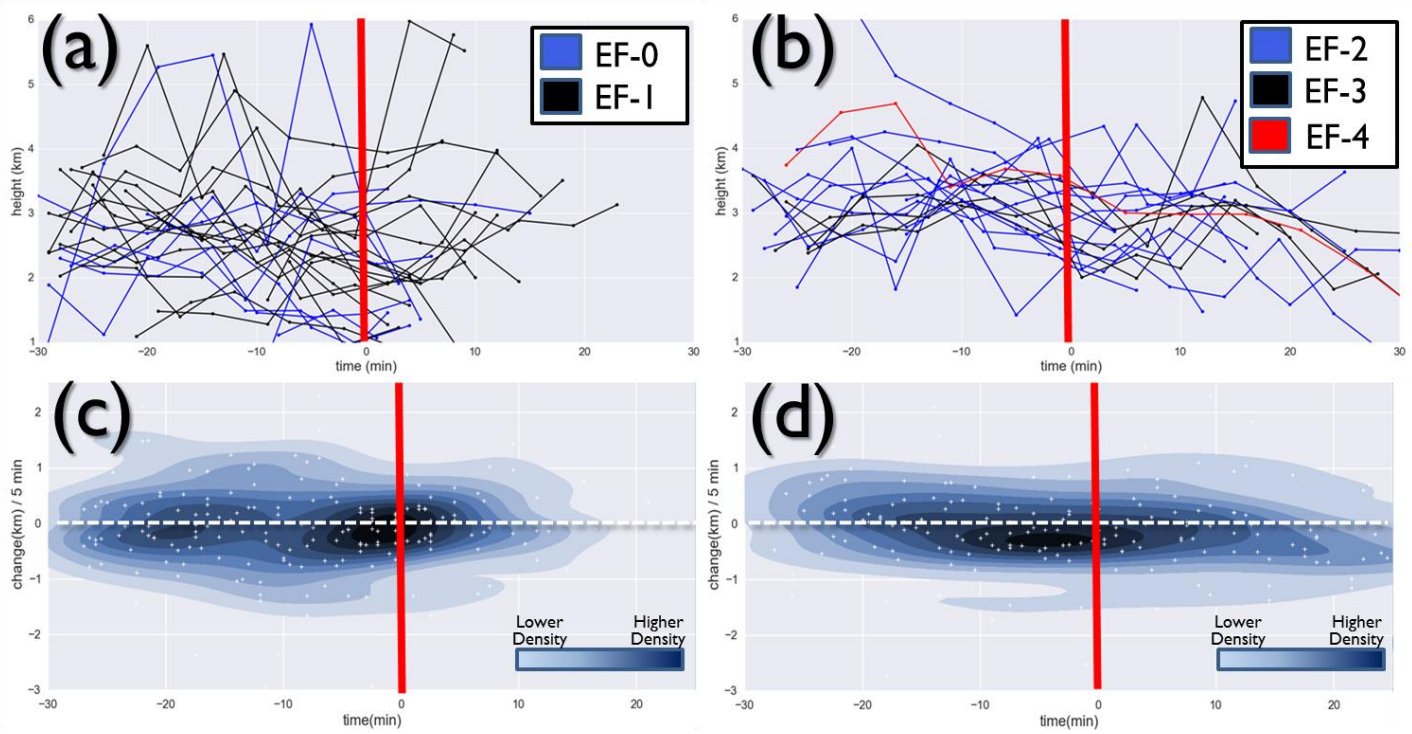

Fig. 4: a) Time-series trends of Z_{DR} column height for (a) weak tornadoes and (b) significant tornadoes as well as scatterplots (and associated density estimation) of the column height change per five minutes for (c) weak tornadoes and (d) significant tornadoes. The vertical red line in each highlights the time of tornadogenesis.

Time Prior to Tornadogenesis	10 to 5 min	10 to 0 min	5 to 0 min
Column Decrease (Weak)	14 (-562 m)	17 (-578 m)	17 (-539 m)
Column Increase (Weak)	9 (783 m)	6 (859 m)	10 (221 m)
Column Decrease (Sig)	12 (-460 m)	14 (-646 m)	14 (-410 m)
Column Increase (Sig)	6 (253 m)	4 (198 m)	4 (371 m)

Table 1: The number of cases that exhibited increasing/decreasing Z_{DR} column trends for weak and significant tornadoes at three time ranges prior to tornadogenesis. The mean value of the change for each group is provided in parentheses. Note: Not all weak tornado cases are included for the 10-to-5 and 10-to-0 min groups as Z_{DR} columns could only be successfully matched to the respective tornado within 10 minutes of development.

Future studies should compare Z_{DR} column depth trends with trends in low-level rotational velocity, as this would be a more direct test of the hypothesis. Additionally, non-tornadic supercell cases should be analyzed for the development of a robust null set. Lastly, instead of using a maximum column height, a volumetric approach to the Z_{DR} column (i.e., counting grid boxes with Z_{DR} above a certain threshold) may be less prone to fluctuations, providing a clearer estimate of updraft trends. Moreover, such a methodology may improve trend estimates for strongly tilted updrafts in high-shear environments.

5. Acknowledgements

The authors thank Darrel Kingfield of the National Severe Storms Laboratory for his assistance with data processing in the WDSSII framework. Additionally, Israel Jirak, Steve Weiss, and Roger Edwards (Storm Prediction Center) are acknowledged for providing constructive feedback enhancing this work.

6. References

Adlerman, E.J., K.K. Droegemeier, and R.P. Davies-Jones, 1999: A numerical simulation of cyclic mesocyclogenesis. *J. Atmos. Sci.*, **56**, 2045-2069.

Brandes, E.A., 1978: Mesocyclone evolution and tornadogenesis: Some observations. *Mon. Wea. Rev.*, **106**, 995-1011.

Caylor, I.C., and A.J. Illingworth, 1987: Radar observations and modeling of warm rain initiation. *Quart. J. Roy. Meteor. Soc.*, **113**, 1171-1191.

Hall, M. P. M., J. W. F. Goddard, and S. M. Cherry, 1984: Identification of hydrometeors and other targets by dual-polarization radar. *Radio. Sci.*, **19**, 132–140.

Houze, R.A., 1993: *Cloud Dynamics*. Academic Press, 573 pp.

Illingworth, A.J., J.F. Goddard, and S.M. Cherry, 1987: Polarization radar studies of precipitation development in convective storms. *Quart. J. Roy. Meteor. Soc.*, **113**, 469-489.

Lemon, L.R., and C.A. Doswell, 1979: Severe thunderstorm evolution and mesocyclone structure as related to

tornadogenesis. *Mon. Wea. Rev.*, **107**, 1184-1197.

Kumjian, M.R., S. Ganson, and A.V. Ryzhkov, 2012: Raindrop freezing in deep convective updrafts: Polarimetric and microphysical model. *J. Atmos. Sci.,* **69***,* 3471-3490.

Kumjian, M.R., A.P. Khain, N. Benmoshe, E. Ilotoviz, A.V. Ryzhkov, and V.T.J. Phillips, 2014: The anatomy and physics of ZDR columns: Investigating a polarimetric radar signature with a spectral bin microphysical model. *J. Appl. Meteor. Climatol.*, **53**, 1820–1843.

Picca, J.C., M. R. Kumjian, and A. V. Ryzhkov, 2010: ZDR columns as a predictive tool for hail growth and storm evolution. Pre-prints, 25th Conf. on Severe Local Storms, Denver, CO, Amer. Meteor. Soc., 11.3. [Available online at https://ams.confex.com/ams/25SLS/webprogram/Paper175750.html.]

Pruppacher, H. R., and J. D. Klett, 1997: Microphysics of Clouds and Precipitation. 2nd ed. Kluwer Academic, 954 pp.

Snyder, J.C., A.V. Ryzhkov, M.R. Kumjian, A.P. Khain, and J. Picca, 2015: A ZDR column detection algorithm to examine convective storm updrafts. *Wea. Forecasting*, **conditionally accepted**.

Trapp, R.J., 1999: Observations of nontornadic low-level mesocyclones and attendant tornadogenesis failure during VORTEX. *Mon. Wea. Rev.*, **127**, 1963-1705.